

Search for $D^0 - \overline{D}^0$ mixing using semileptonic decays at Belle

K. Abe,⁹ K. Abe,⁴⁷ I. Adachi,⁹ H. Aihara,⁴⁹ K. Aoki,²³ K. Arinstein,² Y. Asano,⁵⁴
 T. Aso,⁵³ V. Aulchenko,² T. Aushev,¹³ T. Aziz,⁴⁵ S. Bahinipati,⁵ A. M. Bakich,⁴⁴
 V. Balagura,¹³ Y. Ban,³⁶ S. Banerjee,⁴⁵ E. Barberio,²² M. Barbero,⁸ A. Bay,¹⁹ I. Bedny,²
 U. Bitenc,¹⁴ I. Bizjak,¹⁴ S. Blyth,²⁵ A. Bondar,² A. Bozek,²⁹ M. Bračko,^{9,21,14}
 J. Brodzicka,²⁹ T. E. Browder,⁸ M.-C. Chang,⁴⁸ P. Chang,²⁸ Y. Chao,²⁸ A. Chen,²⁵
 K.-F. Chen,²⁸ W. T. Chen,²⁵ B. G. Cheon,⁴ C.-C. Chiang,²⁸ R. Chistov,¹³ S.-K. Choi,⁷
 Y. Choi,⁴³ Y. K. Choi,⁴³ A. Chuvikov,³⁷ S. Cole,⁴⁴ J. Dalseno,²² M. Danilov,¹³ M. Dash,⁵⁶
 L. Y. Dong,¹¹ R. Dowd,²² J. Dragic,⁹ A. Drutskoy,⁵ S. Eidelman,² Y. Enari,²³ D. Epifanov,²
 F. Fang,⁸ S. Fratina,¹⁴ H. Fujii,⁹ N. Gabyshev,² A. Garmash,³⁷ T. Gershon,⁹ A. Go,²⁵
 G. Gokhroo,⁴⁵ P. Goldenzweig,⁵ B. Golob,^{20,14} A. Gorišek,¹⁴ M. Grosse Perdekamp,³⁸
 H. Guler,⁸ R. Guo,²⁶ J. Haba,⁹ K. Hara,⁹ T. Hara,³⁴ Y. Hasegawa,⁴² N. C. Hastings,⁴⁹
 K. Hasuko,³⁸ K. Hayasaka,²³ H. Hayashii,²⁴ M. Hazumi,⁹ T. Higuchi,⁹ L. Hinz,¹⁹ T. Hojo,³⁴
 T. Hokuue,²³ Y. Hoshi,⁴⁷ K. Hoshina,⁵² S. Hou,²⁵ W.-S. Hou,²⁸ Y. B. Hsiung,²⁸
 Y. Igarashi,⁹ T. Iijima,²³ K. Ikado,²³ A. Imoto,²⁴ K. Inami,²³ A. Ishikawa,⁹ H. Ishino,⁵⁰
 K. Itoh,⁴⁹ R. Itoh,⁹ M. Iwasaki,⁴⁹ Y. Iwasaki,⁹ C. Jacoby,¹⁹ C.-M. Jen,²⁸ R. Kagan,¹³
 H. Kakuno,⁴⁹ J. H. Kang,⁵⁷ J. S. Kang,¹⁶ P. Kapusta,²⁹ S. U. Kataoka,²⁴ N. Katayama,⁹
 H. Kawai,³ N. Kawamura,¹ T. Kawasaki,³¹ S. Kazi,⁵ N. Kent,⁸ H. R. Khan,⁵⁰
 A. Kibayashi,⁵⁰ H. Kichimi,⁹ H. J. Kim,¹⁸ H. O. Kim,⁴³ J. H. Kim,⁴³ S. K. Kim,⁴¹
 S. M. Kim,⁴³ T. H. Kim,⁵⁷ K. Kinoshita,⁵ N. Kishimoto,²³ S. Korpar,^{21,14} Y. Kozakai,²³
 P. Križan,^{20,14} P. Krokovny,⁹ T. Kubota,²³ R. Kulasiri,⁵ C. C. Kuo,²⁵ H. Kurashiro,⁵⁰
 E. Kurihara,³ A. Kusaka,⁴⁹ A. Kuzmin,² Y.-J. Kwon,⁵⁷ J. S. Lange,⁶ G. Leder,¹²
 S. E. Lee,⁴¹ Y.-J. Lee,²⁸ T. Lesiak,²⁹ J. Li,⁴⁰ A. Limosani,⁹ S.-W. Lin,²⁸ D. Liventsev,¹³
 J. MacNaughton,¹² G. Majumder,⁴⁵ F. Mandl,¹² D. Marlow,³⁷ H. Matsumoto,³¹
 T. Matsumoto,⁵¹ A. Matyja,²⁹ Y. Mikami,⁴⁸ W. Mitaroff,¹² K. Miyabayashi,²⁴ H. Miyake,³⁴
 H. Miyata,³¹ Y. Miyazaki,²³ R. Mizuk,¹³ D. Mohapatra,⁵⁶ G. R. Moloney,²² T. Mori,⁵⁰
 A. Murakami,³⁹ T. Nagamine,⁴⁸ Y. Nagasaka,¹⁰ T. Nakagawa,⁵¹ I. Nakamura,⁹
 E. Nakano,³³ M. Nakao,⁹ H. Nakazawa,⁹ Z. Natkaniec,²⁹ K. Neichi,⁴⁷ S. Nishida,⁹
 O. Nitoh,⁵² S. Noguchi,²⁴ T. Nozaki,⁹ A. Ogawa,³⁸ S. Ogawa,⁴⁶ T. Ohshima,²³ T. Okabe,²³
 S. Okuno,¹⁵ S. L. Olsen,⁸ Y. Onuki,³¹ W. Ostrowicz,²⁹ H. Ozaki,⁹ P. Pakhlov,¹³ H. Palka,²⁹
 C. W. Park,⁴³ H. Park,¹⁸ K. S. Park,⁴³ N. Parslow,⁴⁴ L. S. Peak,⁴⁴ M. Pernicka,¹²
 R. Pestotnik,¹⁴ M. Peters,⁸ L. E. Piilonen,⁵⁶ A. Poluektov,² F. J. Ronga,⁹ N. Root,²
 M. Rozanska,²⁹ H. Sahoo,⁸ M. Saigo,⁴⁸ S. Saitoh,⁹ Y. Sakai,⁹ H. Sakamoto,¹⁷
 H. Sakaue,³³ T. R. Sarangi,⁹ M. Satapathy,⁵⁵ N. Sato,²³ N. Satoyama,⁴² T. Schietinger,¹⁹
 O. Schneider,¹⁹ P. Schönmeier,⁴⁸ J. Schümman,²⁸ C. Schwanda,¹² A. J. Schwartz,⁵
 T. Seki,⁵¹ K. Senyo,²³ R. Seuster,⁸ M. E. Sevier,²² T. Shibata,³¹ H. Shibuya,⁴⁶
 J.-G. Shiu,²⁸ B. Shwartz,² V. Sidorov,² J. B. Singh,³⁵ A. Somov,⁵ N. Soni,³⁵ R. Stamen,⁹
 S. Stanič,³² M. Starič,¹⁴ A. Sugiyama,³⁹ K. Sumisawa,⁹ T. Sumiyoshi,⁵¹ S. Suzuki,³⁹
 S. Y. Suzuki,⁹ O. Tajima,⁹ N. Takada,⁴² F. Takasaki,⁹ K. Tamai,⁹ N. Tamura,³¹
 K. Tanabe,⁴⁹ M. Tanaka,⁹ G. N. Taylor,²² Y. Teramoto,³³ X. C. Tian,³⁶ K. Trabelsi,⁸

Y. F. Tse,²² T. Tsuboyama,⁹ T. Tsukamoto,⁹ K. Uchida,⁸ Y. Uchida,⁹ S. Uehara,⁹
T. Uglov,¹³ K. Ueno,²⁸ Y. Unno,⁹ S. Uno,⁹ P. Urquijo,²² Y. Ushiroda,⁹ G. Varner,⁸
K. E. Varvell,⁴⁴ S. Villa,¹⁹ C. C. Wang,²⁸ C. H. Wang,²⁷ M.-Z. Wang,²⁸ M. Watanabe,³¹
Y. Watanabe,⁵⁰ L. Widhalm,¹² C.-H. Wu,²⁸ Q. L. Xie,¹¹ B. D. Yabsley,⁵⁶ A. Yamaguchi,⁴⁸
H. Yamamoto,⁴⁸ S. Yamamoto,⁵¹ Y. Yamashita,³⁰ M. Yamauchi,⁹ Heyoung Yang,⁴¹
J. Ying,³⁶ S. Yoshino,²³ Y. Yuan,¹¹ Y. Yusa,⁴⁸ H. Yuta,¹ S. L. Zang,¹¹ C. C. Zhang,¹¹
J. Zhang,⁹ L. M. Zhang,⁴⁰ Z. P. Zhang,⁴⁰ V. Zhilich,² T. Ziegler,³⁷ and D. Zürcher¹⁹

(The Belle Collaboration)

¹*Aomori University, Aomori*

²*Budker Institute of Nuclear Physics, Novosibirsk*

³*Chiba University, Chiba*

⁴*Chonnam National University, Kwangju*

⁵*University of Cincinnati, Cincinnati, Ohio 45221*

⁶*University of Frankfurt, Frankfurt*

⁷*Gyeongsang National University, Chinju*

⁸*University of Hawaii, Honolulu, Hawaii 96822*

⁹*High Energy Accelerator Research Organization (KEK), Tsukuba*

¹⁰*Hiroshima Institute of Technology, Hiroshima*

¹¹*Institute of High Energy Physics,*

Chinese Academy of Sciences, Beijing

¹²*Institute of High Energy Physics, Vienna*

¹³*Institute for Theoretical and Experimental Physics, Moscow*

¹⁴*J. Stefan Institute, Ljubljana*

¹⁵*Kanagawa University, Yokohama*

¹⁶*Korea University, Seoul*

¹⁷*Kyoto University, Kyoto*

¹⁸*Kyungpook National University, Taegu*

¹⁹*Swiss Federal Institute of Technology of Lausanne, EPFL, Lausanne*

²⁰*University of Ljubljana, Ljubljana*

²¹*University of Maribor, Maribor*

²²*University of Melbourne, Victoria*

²³*Nagoya University, Nagoya*

²⁴*Nara Women's University, Nara*

²⁵*National Central University, Chung-li*

²⁶*National Kaohsiung Normal University, Kaohsiung*

²⁷*National United University, Miao Li*

²⁸*Department of Physics, National Taiwan University, Taipei*

²⁹*H. Niewodniczanski Institute of Nuclear Physics, Krakow*

³⁰*Nippon Dental University, Niigata*

³¹*Niigata University, Niigata*

³²*Nova Gorica Polytechnic, Nova Gorica*

³³*Osaka City University, Osaka*

³⁴*Osaka University, Osaka*

³⁵*Panjab University, Chandigarh*

³⁶*Peking University, Beijing*

³⁷*Princeton University, Princeton, New Jersey 08544*

³⁸*RIKEN BNL Research Center, Upton, New York 11973*

³⁹*Saga University, Saga*

⁴⁰*University of Science and Technology of China, Hefei*

⁴¹*Seoul National University, Seoul*

⁴²*Shinshu University, Nagano*

⁴³*Sungkyunkwan University, Suwon*

⁴⁴*University of Sydney, Sydney NSW*

⁴⁵*Tata Institute of Fundamental Research, Bombay*

⁴⁶*Toho University, Funabashi*

⁴⁷*Tohoku Gakuin University, Tagajo*

⁴⁸*Tohoku University, Sendai*

⁴⁹*Department of Physics, University of Tokyo, Tokyo*

⁵⁰*Tokyo Institute of Technology, Tokyo*

⁵¹*Tokyo Metropolitan University, Tokyo*

⁵²*Tokyo University of Agriculture and Technology, Tokyo*

⁵³*Toyama National College of Maritime Technology, Toyama*

⁵⁴*University of Tsukuba, Tsukuba*

⁵⁵*Utkal University, Bhubaneswer*

⁵⁶*Virginia Polytechnic Institute and State University, Blacksburg, Virginia 24061*

⁵⁷*Yonsei University, Seoul*

Abstract

A search for mixing in the neutral D meson system has been performed using semileptonic $D^0 \rightarrow K^{(*)-} e^+ \nu$ decays. Neutral D mesons from $D^{*+} \rightarrow D^0 \pi^+$ decays are used; the flavor at production is tagged by the charge of the slow pion. The measurement is performed using 253 fb^{-1} of data recorded by the Belle detector. From the yield of right-sign and wrong-sign decays arising from non-mixed and mixed events, respectively, we estimate the upper limit of the time-integrated mixing rate to be $r_D < 1.0 \times 10^{-3}$ at 90% C.L.

PACS numbers: 14.40.Lb, 13.20.Fc, 12.15.Ff, 11.30.Er

I. INTRODUCTION

The phenomenon of mixing has been observed in the $K^0 - \bar{K}^0$ and $B^0 - \bar{B}^0$ systems, but not yet in the $D^0 - \bar{D}^0$ system. The rate of $D^0 - \bar{D}^0$ mixing within the Standard Model is expected to be small [1].

The parameters used to characterize the mixing are $x = \Delta m/\bar{\Gamma}$ and $y = \Delta\Gamma/2\bar{\Gamma}$, where Δm and $\Delta\Gamma$ are the differences in mass and decay width between the two neutral charmed meson mass eigenstates, and $\bar{\Gamma}$ is the mean decay width. For $x, y \ll 1$ and negligible CP violation, the time-dependent mixing probability for semileptonic D^0 decays is [2]

$$\mathcal{P}(D^0 \rightarrow \bar{D}^0 \rightarrow X^+ \ell^- \bar{\nu}_\ell) \propto r_D t^2 e^{-\Gamma t} \quad (1)$$

where r_D is the ratio of the time-integrated mixing to the time-integrated non-mixing probability:

$$r_D = \frac{\int_0^\infty dt \mathcal{P}(D^0 \rightarrow \bar{D}^0 \rightarrow X^+ \ell^- \bar{\nu}_\ell)}{\int_0^\infty dt \mathcal{P}(D^0 \rightarrow X^- \ell^+ \nu_\ell)} \approx \frac{x^2 + y^2}{2} \quad (2)$$

In this paper we present a search for $D^0 - \bar{D}^0$ mixing using semileptonic decays of charmed mesons. The flavor of a neutral D meson at production is determined from the charge of the accompanying slow pion (π_s) in the $D^{*+} \rightarrow D^0 \pi_s^+$ decay [3]. We reconstruct the D^0 as $D^0 \rightarrow K^{(*)-} e^+ \nu_e$ and identify its flavor at the time of decay from the charge correlation of the kaon and the electron. We search for mixing by reconstructing the ‘‘wrong sign’’ (WS) decay chain, $D^{*+} \rightarrow D^0 \pi_s^+$, $D^0 \rightarrow \bar{D}^0$, $\bar{D}^0 \rightarrow K^{(*)+} e^- \bar{\nu}_e$, which results in a WS charge combination of three of the particles used in reconstruction, $\pi_s^+ K^+ e^-$. The non-mixed process results in a ‘‘right sign’’ (RS) charge combination, $\pi_s^+ K^- e^+$. In contrast to hadronic decays, the WS charge combinations can occur only through mixing, and r_D can be obtained directly as the ratio of WS to RS signal events.

We make no attempt to reconstruct K^{*-} mesons. We treat charged daughter particles (K^- or π^-) as if they were the direct daughters of the D^0 , omitting the accompanying neutral particle. A small contribution from $D^0 \rightarrow \rho^-/\pi^- e^+ \nu_e$ modes is also included (without reconstructing the rho mesons) if the charged pion survives the kaon selection criteria.

We measure r_D in a 253 fb^{-1} data sample recorded by the Belle detector at the KEKB asymmetric e^+e^- collider [4], at a center-of-mass (cms) energy of about 10.6 GeV. The Belle detector [5] is a large-solid-angle magnetic spectrometer that consists of a silicon vertex detector (SVD), a 50-layer central drift chamber (CDC), an array of aerogel threshold Čerenkov counters (ACC), a barrel-like arrangement of time-of-flight scintillation counters (TOF), and an electromagnetic calorimeter (ECL) comprised of CsI(Tl) crystals located inside a superconducting solenoid coil that provides a 1.5 T magnetic field. An iron flux-return located outside of the coil is instrumented to detect K_L^0 mesons and to identify muons (KLM). Two different inner detector configurations were used. The first 140 fb^{-1} of data were taken using a 2.0 cm radius beampipe and a 3-layer silicon vertex detector and the latter 113 fb^{-1} using a 1.5 cm radius beampipe, a 4-layer silicon detector and a small-cell inner drift chamber [6].

Simulated events are generated by the QQ generator and processed with a full simulation of the Belle detector, using the GEANT package [7]. To simulate mixed D meson decays we use generic (non-mixed) Monte Carlo (MC) events and appropriately reweight the proper decay time distribution.

II. SELECTION AND RECONSTRUCTION

For π_s^+ candidates we consider tracks with momentum $p < 600 \text{ MeV}/c$; projections of the impact parameter with respect to the interaction point in the radial and beam directions $dr < 1 \text{ cm}$ and $|dz| < 2 \text{ cm}$, respectively; and electron identification likelihood, based on the information from the CDC, ACC and ECL [8], $\mathcal{L}_e < 0.1$. Electron candidates are required to have $p > 600 \text{ MeV}/c$ and $\mathcal{L}_e > 0.95$. Kaon candidates are chosen from the remaining tracks in the event with $p > 800 \text{ MeV}/c$ and $\mathcal{L}(K^\pm)/(\mathcal{L}(K^\pm) + \mathcal{L}(\pi^\pm)) > 0.5$, where $\mathcal{L}(K^\pm, \pi^\pm)$ is the likelihood that a given track is a K^\pm or a π^\pm , based on information from the TOF, CDC and ACC [9]. Charged pions originating from semileptonic $D^0 \rightarrow \pi^- e^+ \nu$ decays which pass the kaon selection criteria are treated as kaons and assigned the kaon mass. According to MC simulation this selection retains about 58% (43%, 52%) of signal slow pions (electrons, kaons), and at this stage about 13% (5%, 44%) of the selected π_s (e, K) candidates are misidentified.

The variable used to isolate the signal events is $\Delta M = M(\pi_s K e \nu_e) - M(K e \nu_e)$, where $M(\pi_s K e \nu_e)$ and $M(K e \nu_e)$ are the invariant masses of the selected charged particles and reconstructed neutrino, with and without the slow pion.

We require the cms momentum of the kaon-electron system to be $p_{\text{cms}}(Ke) > 2 \text{ GeV}/c$ to reduce the combinatorial background and the background from $B\bar{B}$ events, and to improve the resolution in ΔM . To further suppress the contribution of $B\bar{B}$ events, we required the ratio of the second to the zeroth Fox-Wolfram moments, known as R_2 , to be greater than 0.2 [10].

Background from $D^0 \rightarrow K^- \pi^+$ is suppressed by requiring the invariant mass of the K - e system to satisfy $M(Ke) < 1.82 \text{ GeV}/c^2$. Background from $D^0 \rightarrow K^- K^+$ is effectively reduced by the requirement $|M(KK) - m_{D^0}| > 10 \text{ MeV}/c^2$, where $M(KK)$ is the K - e invariant mass, calculated using the kaon mass for both tracks.

Electron pairs from photon conversions, which can be misidentified as the electron and slow pion candidates, are suppressed by requiring $M(e^+e^-) > 150 \text{ MeV}/c^2$, where $M(e^+e^-)$ is the invariant mass of the π_s^+ - e^- system with the electron mass assigned to the pion. A further search for an additional e^\pm with charge opposite to that of the electron (slow pion) candidate in the D^{*+} (D^0) decay is performed in each event. Candidates with $M(e^+e^-)$ below $150 \text{ MeV}/c^2$ are rejected.

The first approximation of the neutrino four-momentum is calculated from four-momentum conservation:

$$P_\nu = P_{\text{cms}} - P_{\pi_s Ke} - P_{\text{rest}} \quad (3)$$

where P_{cms} denotes the cms four-momentum of the e^+e^- system, $P_{\pi_s Ke}$ the cms four-momentum of the π_s - K - e combination, and P_{rest} the cms four-momenta of all the charged tracks and photons in the event, excluding the slow pion, kaon and electron candidates. The ΔM resolution is significantly improved by applying two kinematic constraints to correct P_{rest} . First, events with $-4 \text{ GeV}^2/c^4 < M(\pi_s Ke \nu)^2 < 36 \text{ GeV}^2/c^4$ are selected and the magnitude of P_{rest} is rescaled by a factor x such that $M(\pi_s Ke \nu)^2 = (P_{\text{cms}} - x P_{\text{rest}})^2 \equiv m_{D^{*\pm}}^2$, with $m_{D^{*\pm}}$ fixed to its nominal value [11]. Next, only events with $-2 \text{ GeV}^2/c^4 < M_\nu^2 < 0.5 \text{ GeV}^2/c^4$ are retained and the direction of the three-momentum \mathbf{p}_{rest} is corrected in order to yield $M_\nu^2 \equiv 0$. The correction rotates \mathbf{p}_{rest} in the plane determined by the vectors \mathbf{p}_{rest} and $\mathbf{p}_{\pi_s Ke}$.

The mass difference ΔM is then calculated using this reconstructed neutrino four-momentum. The full width at half maximum (FWHM) of the ΔM peak in MC simulated

$D^0 \rightarrow K^- e^+ \nu$ events is found to be $7 \text{ MeV}/c^2$. Events with $\Delta M < 0.18 \text{ GeV}/c^2$ are retained for further analysis.

According to MC simulation, the $D^0 \rightarrow K^{*-} e^+ \nu_e$ and $D^0 \rightarrow \rho^- / \pi^- e^+ \nu_e$ modes have similar ΔM distributions to that of the $D^0 \rightarrow K^- e^+ \nu_e$ decay, but with a larger FWHM. The charge correlation is preserved if the slow pion decays into a muon, and the muon is taken as the slow pion candidate. These decays will be referred to as ‘‘associated signal’’ decays. Their fraction in the reconstructed MC signal sample was found to be $14.9 \pm 0.1\%$, with the quoted error being due to MC statistics only.

According to MC, the backgrounds for both RS and WS decays consist mainly of combinatorial background (98.4% and 98.0%, respectively). In order to minimize systematic uncertainties, we model the shape of this background using data. We use the ‘‘combinatorial sign’’ (CS) of $\pi_s^+ K^- e^-$ or $\pi_s^+ K^+ e^+$ to model the combinatorial background in the RS sample. In the WS sample this background is due to random π_s^+ candidates combined with the selected kaon and electron candidates, and is modelled by combining π_s^+ and $(K^- + e^+)$ candidates from different events. The correlated background in the RS sample (1.6%) comes mainly from $D^0 \rightarrow K^- \pi^+ \pi^0$ decays in which the π^+ is misidentified as an e^+ . The correlated background in the WS sample (2.0%) is composed of combinations in which the π_s^+ candidate is a true π_s^+ from a D^{*+} decay, but either the kaon or the electron candidate (or both, with at least one being misidentified) are from the corresponding D^0 decay. This background is described using MC.

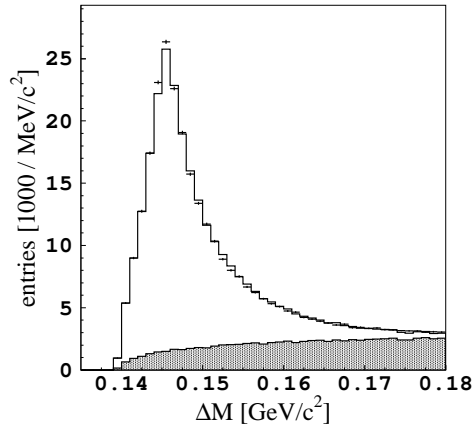


FIG. 1: ΔM distribution for RS events. The data (background) is represented by points with error bars (hatched histogram), and the result of the binned maximum likelihood fit by the solid line.

Figure 1 shows the ΔM distribution for RS events. We perform a binned maximum likelihood fit to the distribution, maximizing

$$\mathcal{L} = \prod_{i=1}^{N_{bin}} \frac{e^{-\mu(\Delta M_i)} \times (\mu(\Delta M_i))^{N_i}}{N_i!} \quad (4)$$

where N_i is the number of entries in the i -th bin and $\mu(\Delta M_i)$ is the expected number of events in this bin, given by

$$\mu(\Delta M_i) = \mathcal{N}[f_s P_s(\Delta M_i) + (1 - f_s) P_b(\Delta M_i)] \quad (5)$$

P_s (P_b) is the signal (background) ΔM distribution obtained from MC (as described above); f_s and \mathcal{N} are the signal fraction and the overall normalization, respectively, and are free parameters in the fit. The hatched histogram in Figure 1 shows the fitted background contribution. The fitted signal fraction is $f_s = 73.4 \pm 0.1\%$ and the number of RS signal events is $N_{RS}^{tot} = 229,452 \pm 597$.

We increase the sensitivity to $D^0 - \overline{D^0}$ mixing by exploiting the measurement of the D^0 proper decay time. The decay time is evaluated using the measured momentum of the meson and the distance from the e^+e^- interaction point to the reconstructed D^0 decay $K-e$ vertex. Due to the shape of the KEKB accelerator interaction region, which is narrowest in the vertical (y) direction, the dimensionless proper decay time t_y is calculated as

$$t_y = \frac{m_{D^0}}{c\tau_{D^0}} \frac{y_{\text{vtx}} - y_{\text{IP}}}{p_y} \quad (6)$$

where p_y is the y component of the D^0 candidate's momentum and y_{vtx} and y_{IP} are the y coordinates of the reconstructed $K-e$ vertex and of the interaction point, respectively. m_{D^0} and τ_{D^0} are the nominal mass and lifetime of D^0 mesons [11].

Mixed and non-mixed processes have different proper decay time distributions, modelled by $t^2 e^{-t/\tau_{D^0}}$ and $e^{-t/\tau_{D^0}}$, respectively. In order to calculate the mixing parameter r_D after any selection based on D^0 proper decay time, the ratio of the two types of signal events, N_{WS}/N_{RS} , must be multiplied by the ratio of their efficiencies, $\epsilon_{\text{nonmix}}/\epsilon_{\text{mix}}$. The efficiencies are obtained from the convolution of the above proper decay time distributions with the detector resolution function. As the observed proper decay time distribution is a convolution of the signal and background probability density functions (p.d.f.) with the detector resolution function, the latter can be found by performing a binned χ^2 fit to the RS events' t_y distribution: $\int_0^\infty dt [f_s e^{-t/\tau_{D^0}} + (1 - f_s)(f_e e^{-t/\tau_{bkg}} + (1 - f_e)\delta(t))] \times \mathcal{R}(t/\tau_{D^0} - t_y)$. The signal fraction f_s is obtained from the fit to the ΔM distribution. The fraction f_e of the non-prompt background component and its lifetime τ_{bkg} are fixed to the values obtained by fitting the MC background t_y distributions; $\delta(t)$ describes the shape of the prompt background component. The resolution function $\mathcal{R}(t - t_y)$ is described phenomenologically by the sum of three Gaussians and an additional term for badly reconstructed tracks ("outliers"); we obtain the widths and coefficients from the fit.

The ratios $\epsilon_{\text{nonmix}}/\epsilon_{\text{mix}}$ are calculated by integrating the underlying p.d.f.'s for the RS and WS signal events, convolved with the detector resolution function, over the selected t_y intervals. The values are given in Table I. The errors are obtained by varying each parameter in the proper decay time fit by $\pm 1\sigma$, repeating the fit and recalculating the ratios. Using this method, the majority of systematic errors due to the imperfect description of the decay time distribution cancel out.

Comparison of the expected t_y distribution for WS signal and background events indicates that the figure-of-merit, defined as $N_{WS}^{\text{sig}}/\sqrt{N_{WS}^{\text{bkg}}}$, is optimal for $t_y \geq 1$. Events which satisfy this condition are retained for further analysis.

III. FIT AND RESULTS

We extract the RS and WS signal yields separately in six intervals of t_y . The yields are obtained from binned maximum likelihood fits to ΔM , described by Eq. 4; the WS signal distribution is taken to be the same as the RS. The results are shown in Table I and

Figure 2. We obtain the time-integrated mixing probability ratio in the i -th t_y interval, $r_D^i = N_{WS}^i/N_{RS}^i \times \epsilon_{\text{nonmix}}^i/\epsilon_{\text{mix}}^i$, by multiplying the ratio of WS to RS signal events in each interval by the t_y efficiency ratio. The mixing probability is compatible with zero in all proper decay time intervals (see Figure 3).

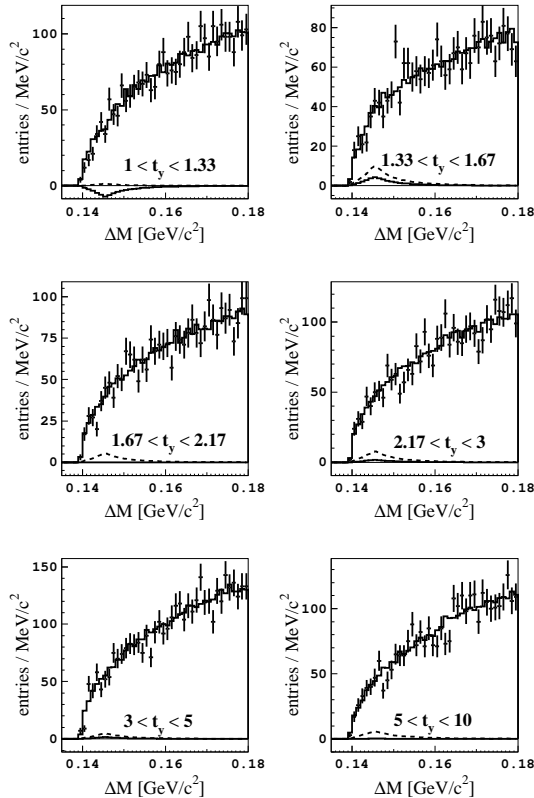


FIG. 2: WS ΔM distributions in six proper decay time intervals for data (points with error bars) and the results of the fit described in the text (solid line). At the bottom of each figure the fitted (expected for $r_D^i = 90\%$ C.L. upper limit) signal yield is plotted as a solid (dashed) line.

The overall r_D follows from a χ^2 fit with a constant to the measured r_D^i values, using a constant:

$$r_D = (0.20 \pm 0.47) \times 10^{-3} \quad (7)$$

The quoted error is statistical only.

IV. SYSTEMATIC UNCERTAINTIES

The experimental procedure was checked using a dedicated MC sample of mixed D^0 decays. These were added in different proportions to the generic MC, which includes both non-mixed D^0 decays and all known types of background decays. Applying the same method

t_y	N_{RS}^i	N_{WS}^i	$\frac{\epsilon_{\text{nonmix}}^i}{\epsilon_{\text{mix}}^i}$	$r_D^i [10^{-3}]$
1 – 1.33	$18\,742 \pm 166$	-63.7 ± 30.2	1.62 ± 0.11	-5.49 ± 2.63
1.33 – 1.67	$15\,032 \pm 147$	40.3 ± 29.9	1.14 ± 0.08	3.05 ± 2.27
1.67 – 2.17	$16\,430 \pm 155$	-1.3 ± 30.6	0.79 ± 0.05	-0.06 ± 1.48
2.17 – 3	$16\,691 \pm 157$	17.0 ± 33.1	0.51 ± 0.03	0.51 ± 1.00
3 – 5	$15\,443 \pm 160$	14.7 ± 37.4	0.30 ± 0.01	0.28 ± 0.72
5 – 10	$8\,263 \pm 123$	3.0 ± 35.2	0.28 ± 0.02	0.10 ± 1.19

TABLE I: The number of fitted signal events in the RS and WS samples, the efficiency ratio $\epsilon_{\text{nonmix}}^i/\epsilon_{\text{mix}}^i$, and the resulting r_D^i value for each proper decay time interval.

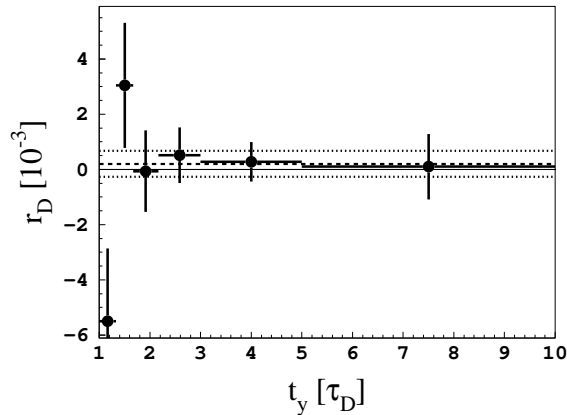


FIG. 3: Measured r_D^i values (points with error bars) in six different proper decay time intervals. The solid (dashed) line shows the null value (the fit to the six r_D^i using a constant). The dotted lines denote the statistical error of the fit.

used for the data on such samples, it was verified that the reconstructed r_D value reproduces the input value without any significant bias.

The main source of systematic error is the limited statistics of the fitting distributions, predominantly the background distribution in the WS sample. To estimate this uncertainty, we vary the contents of all bins of the RS and WS $P_s(\Delta M)$ and $P_b(\Delta M)$ distributions in accordance with each bin's statistical uncertainty, repeat the fit to the RS and WS data, calculate the corresponding r_D^i in each proper decay time interval, and obtain a new r_D value. Repeating the procedure, the obtained distribution of r_D values has a Gaussian distribution with a width of 0.12×10^{-3} , which is taken as the systematic error due to the limited statistics of the fitting distributions.

To estimate the systematic uncertainty due to the ΔM binning and the shape of the WS background, the ΔM distributions in each proper decay time interval, originally divided into 45 bins in the range $0.135 \text{ GeV}/c^2 < \Delta M < 0.180 \text{ GeV}/c^2$, are re-binned into 12, 15, 20, 30 and 60 bins in the same range. The fitting procedure is repeated for each set of bins, and the systematic error due to binning is taken as half the difference between the largest and the smallest r_D : $\pm 0.07 \times 10^{-3}$.

According to MC, the majority of the correlated WS background arises from $D^0 \rightarrow K^- \pi^+ \pi^0$ decays. We repeat the WS fits, changing the amount of this background in accordance with the relative error on $Br(D^0 \rightarrow K^- \pi^+ \pi^0)$. The resulting variation in r_D is $\pm 0.02 \times 10^{-3}$. The same method applied in the fit to the RS sample introduces a negligible variation of the r_D value, less than 0.001×10^{-3} .

We compare $\epsilon_{\text{nonmix}}^i$ values with the corresponding $N_{RS}^i/N_{RS}^{\text{tot}}$ ratios. The relative difference between the two is conservatively assigned as the uncertainty on $\epsilon_{\text{nonmix}}^i/\epsilon_{\text{mix}}^i$, although one expects at least part of the systematic uncertainty to cancel in the efficiency ratio. We simultaneously vary the six efficiency ratios within the limits of this relative difference and repeat the r_D calculation. We quote the difference between the resulting r_D values and the default fit ($\pm 0.02 \times 10^{-3}$) as the systematic error due to an imperfect description of the proper decay time distributions.

The systematic error due to the uncertainty in the associated signal fraction is estimated by varying the fraction and repeating the fitting procedure. Using the errors on the measured branching fractions [11] of the associated signal decay channels, we conservatively vary the amount of associated signal by $\pm 40\%$. We recalculate r_D and compare it to the default r_D value; we quote the difference, 0.002×10^{-3} , as the systematic error from this source.

The quadratic sum of these individual contributions yields a total systematic error of $\pm 0.14 \times 10^{-3}$.

V. CONCLUSION

In summary, we have searched for $D^0 - \overline{D}^0$ mixing in semileptonic D^0 decays. We independently measure the mixing ratios r_D^i in six D^0 proper decay time intervals. By fitting a constant to these six values we obtain the final result

$$r_D = (0.20 \pm 0.47 \pm 0.14) \times 10^{-3} \quad (8)$$

where the first error is the statistical and the second the systematic uncertainty. As we do not observe a significant number of WS D^0 decays, we obtain an upper limit for the time-integrated mixing rate. We use the Feldman-Cousins approach [12] to estimate the upper limit in the vicinity of the physics region boundary ($r_D \geq 0$), and calculate the upper limit from the r_D result in Eq. 8, using the total error. This yields

$$r_D \leq 1.0 \times 10^{-3} \quad \text{at 90\% C.L.} \quad (9)$$

This result is the most stringent experimental limit on the time-integrated D^0 mixing rate obtained to date from semileptonic D^0 decays.

ACKNOWLEDGMENTS

We thank the KEKB group for the excellent operation of the accelerator, the KEK cryogenics group for the efficient operation of the solenoid, and the KEK computer group and the National Institute of Informatics for valuable computing and Super-SINET network support. We acknowledge support from the Ministry of Education, Culture, Sports, Science, and Technology of Japan and the Japan Society for the Promotion of Science; the Australian Research Council and the Australian Department of Education, Science and Training; the National Science Foundation of China under contract No. 10175071; the Department of Science and Technology of India; the BK21 program of the Ministry of Education of Korea

and the CHEP SRC program of the Korea Science and Engineering Foundation; the Polish State Committee for Scientific Research under contract No. 2P03B 01324; the Ministry of Science and Technology of the Russian Federation; the Ministry of Higher Education, Science and Technology of the Republic of Slovenia; the Swiss National Science Foundation; the National Science Council and the Ministry of Education of Taiwan; and the U.S. Department of Energy.



- [1] For a review see for example S. Bianco, F.L. Fabbri, D. Benson and I. Bigi, Riv. Nuovo Cim. **26N7**, 1 (2003); also A. Falk *et al.*, Phys. Rev D **69**, 114021 (2004).
- [2] Z.-Z. Xing, Phys. Rev. **D55**, 196 (1997).
- [3] Charge-conjugate modes are implied throughout this paper.
- [4] S. Kurokawa and E. Kikutani, Nucl. Instr. Meth. A **499**, 1 (2003), and other papers included in this volume.
- [5] A. Abhasian *et al.* (Belle), Nucl. Instr. Meth. A **479**, 117 (2002).
- [6] Y. Ushiroda *et al.*, Nucl. Instr. Meth. **A511**, 6 (2003).
- [7] Events are generated with the CLEO QQ generator (see <http://www.lns.cornell.edu/public/CLEO/soft/QQ>); the detector response is simulated with GEANT, R. Brun *et al.*, GEANT 3.21, CERN Report DD/EE/84-1, (1984).
- [8] K. Hanagaki *et al.*, Nucl. Instrum. Meth. **A 485**, 490 (2002).
- [9] K. Abe *et al.*, Belle Collab., Phys. Rev. **D66** 032007 (2002).
- [10] G.C. Fox and S. Wolfram, Phys. Rev. Lett. **41**, 1581 (1978).
- [11] S. Eidelman *et al.*, Phys. Lett. **B 592**, 1 (2004).
- [12] G.J. Feldman and R.D. Cousins, Phys. Rev. **D57**, 3873 (1998).